

THREE-DIMENSIONAL FEATURES OF UNDULAR HYDRAULIC JUMPS

Hubert CHANSON

Dept. of Civil Engineering, The University of Queensland, Brisbane QLD 4072, Australia

1. INTRODUCTION

In open channels, an undular hydraulic jump is a stationary transition from super- to sub-critical flow. It is characterised by the development of regular and irregular free-surface undulations downstream of the jump. A recent study (CHANSON 1993) showed that the flow characteristics are functions of the upstream Froude number, the aspect ratio d_c/W and the inflow conditions. Further, the flow is three-dimensional (e.g. table 2).

With fully-developed inflows, five different flow regimes can be observed. Typical three-dimensional flow patterns include : lateral shock waves, free-surface recirculation, corner recirculation, roller (fig. 1). An important feature of undular jumps with fully-developed inflow is the lateral shock waves developing upstream of the first wave crest (fig. 1). The shock waves intersect slightly downstream of the top of the first wave. Further downstream, the crosswaves are reflected on the sidewalls and continue to propagate over long distances. CHANSON (1993) suggested a major flow redistribution between the start of the shock wave (SW) and the first wave crest (1C).

In this paper, new experiments are presented (table 1). They were performed in the 20-m long glass channel used by CHANSON (1993) and the upstream flows were a fully-developed boundary layer flows. For an aspect ratio $d_c/W = 0.286$, pressure and velocity distributions were recorded on the centreline ($z/W=0.5$), at $z/W = 0.25$ and $z/W = 0.05$ (i.e. near the sidewall) using a Pitot tube. For each position, the measurements were taken upstream of the jump (U/S), at the start of the shock wave (SW), at 1/3-distance between SW and the first wave crest (SW1), at 2/3-distance between SW and 1C (SW2), at the 1st wave crest (1C), 1st wave bottom (1B) and 2nd wave crest (2C) (see fig. 1).

The results provide new information on the three-dimensional flow redistribution immediately upstream of the first wave crest at undular hydraulic jumps with fully-developed inflow conditions.

2. PRESSURE DISTRIBUTIONS

Figure 2 presents dimensionless pressure distributions along the jump on the centreline (fig. 2A), at $z/W=0.25$ (fig. 2B) and near the sidewall (fig. 2C). The data are shown as $P/(\rho_w * g * d)$ versus y/d where P is the pressure and d is the local flow

depth. At the upstream flow location (U/S), the pressure is hydrostatic. But along the jump, the data show explicitly that the pressure distributions are not hydrostatic.

On the channel centreline (fig. 2A), the pressure gradient $\partial P/\partial y$ is less than hydrostatic at the wave crests. And, at each wave trough, the pressure gradient is larger than hydrostatic as observed by CHANSON (1993).

All data indicate that, at each (x, z) -position located upstream of the lateral shock waves, the pressure gradient is larger than hydrostatic. And $\partial P/\partial y$ is less than hydrostatic downstream of the shockwaves : i.e., at $(SW1)_{z/W=0.05}$, $(SW2)_{z/W=0.05}$, $(SW2)_{z/W=0.05}$, $(1C)_{z/W=0.5}$, $(1C)_{z/W=0.25}$, $(1C)_{z/W=0.05}$.

Visual and photographic observations indicate that the free-surface is concave (i.e. curved upwards) upstream of the shockwaves and convex (i.e. $\partial^2 d/\partial x^2 < 0$) downstream of the crosswaves. With such streamline curvatures, the irrotational flow motion theory (e.g. ROUSE 1938, LIGGETT 1994) predicts a similar trend for the pressure distributions. But, at the wave crests, irrotational wave theories predict larger pressure gradient differences than those observed with undular jumps. Undular jump flows are stationary real-fluid flows and ideal-fluid flow theories cannot predict accurately their behaviour.

Fig. 1 - Flow pattern of undular hydraulic jump with fully-developed upstream flow

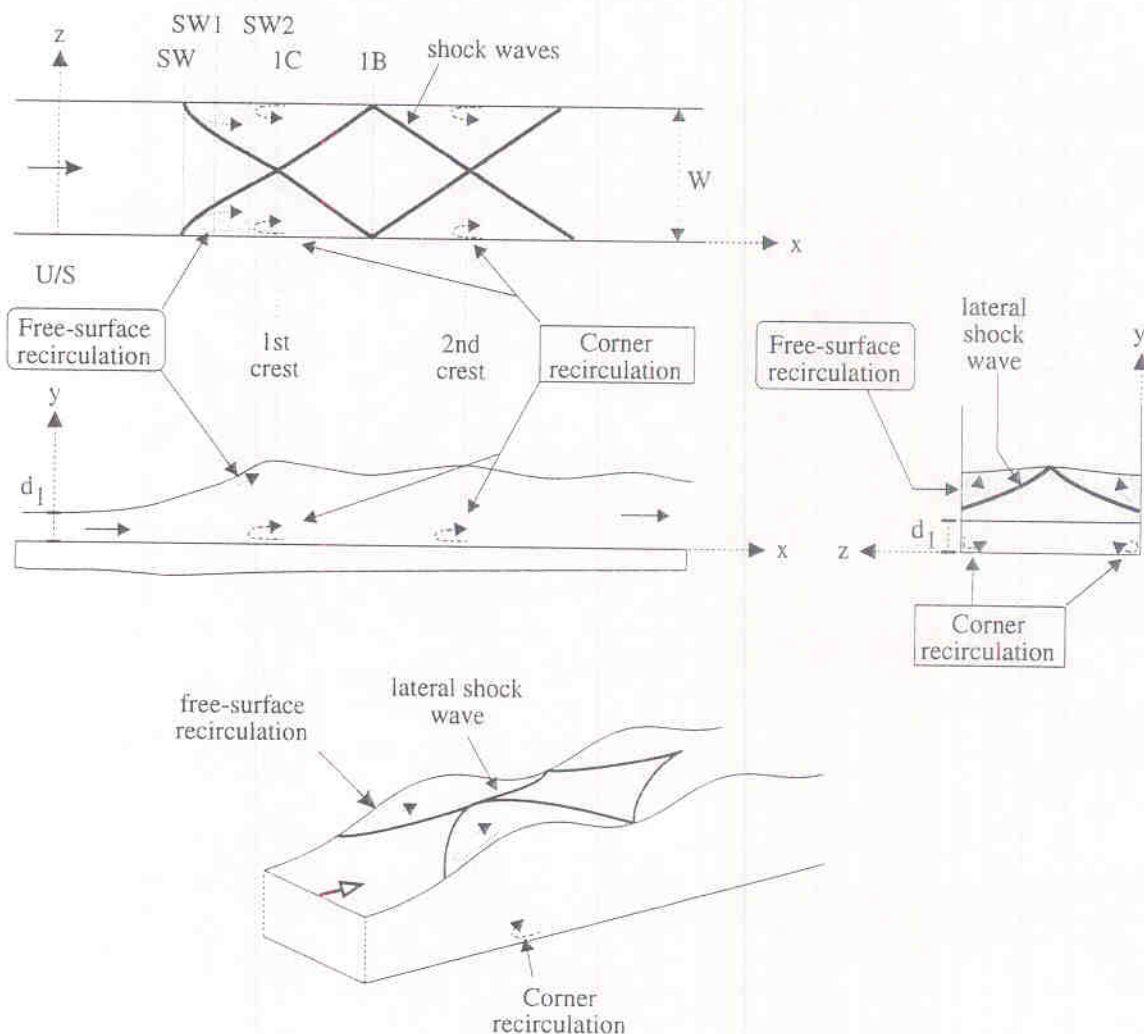


Fig. 2 - Pressure distributions on the centreline, at $z/W = 0.25$ and at $z/W = 0.046$

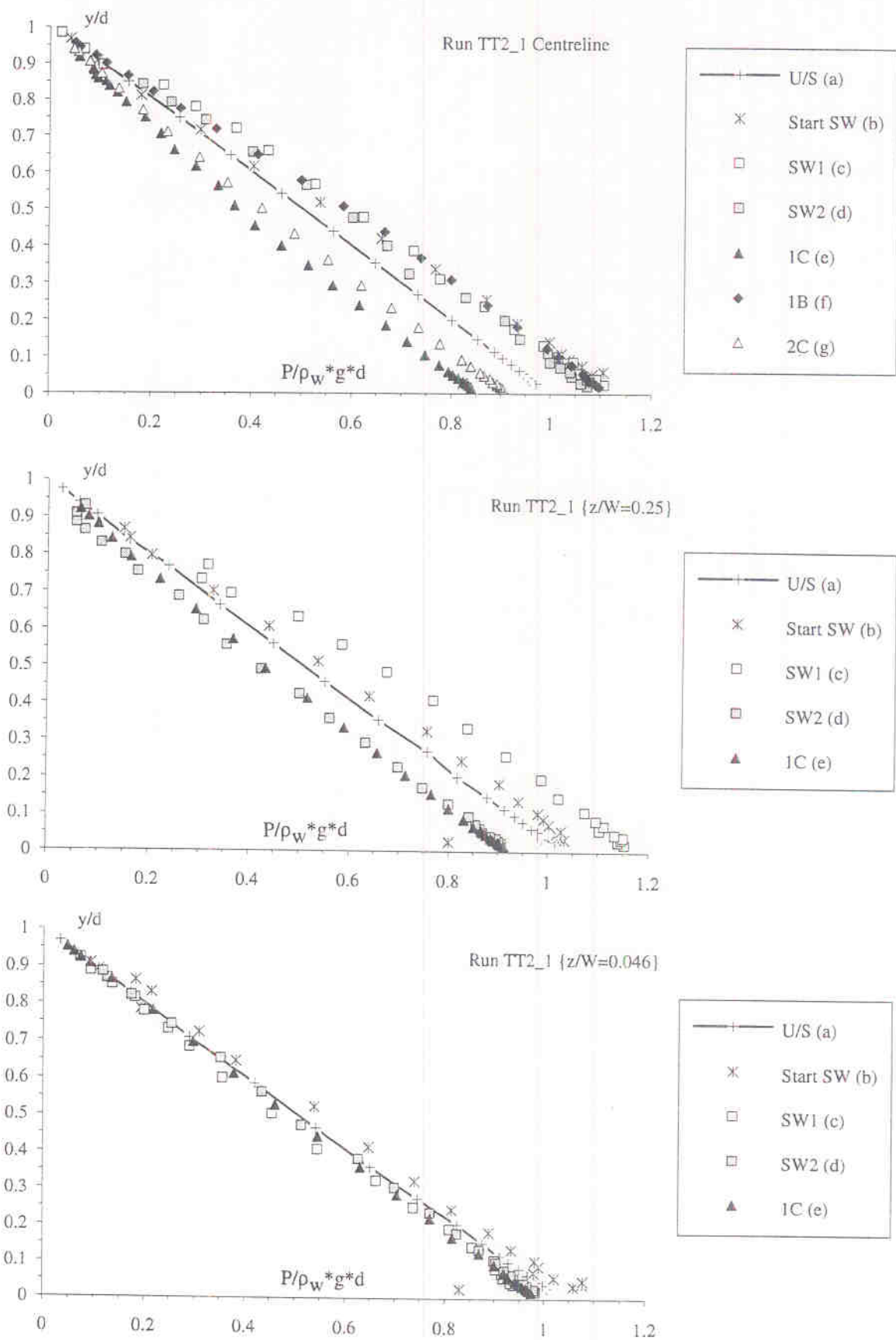


Table 1 - Experimental flow conditions

| Run | q_w (m^2/s) | Fr_1 | x_1 (m) | Jump Type (CHANSON 1993) | Comments |
|-------|----------------------|--------|--------------|-----------------------------|---------------------------------|
| TT2_1 | 0.06 | 1.35 | 10.38 | C | Glass flume. $W = 0.25$ m. |
| TT2_2 | 0.06 | 1.14 | 9.0 | A | Fully-developed upstream flows. |

Table 2 - Free-surface profiles

| Ref. | Run : TT2_1 | | | | Run : TT2_2 | | | |
|------|-------------|-----------|------------|-------------|-------------|-----------|------------|-------------|
| | x (m) | d (m) | | | x (m) | d (m) | | |
| | | $z/W=0.5$ | $z/W=0.25$ | $z/W=0.046$ | | $z/W=0.5$ | $z/W=0.25$ | $z/W=0.054$ |
| U/S | 10.38 | 0.0587 | 0.0582 | 0.0575 | 9.0 | 0.0656 | 0.066 | 0.0664 |
| SW | 10.62 | 0.0618 | 0.0636 | 0.0646 | 10.0 | 0.0666 | 0.0662 | 0.067 |
| SW1 | 10.69 | 0.0724 | 0.0800 | 0.0831 | 10.13 | 0.0674 | 0.0676 | 0.0718 |
| SW2 | 10.75 | 0.0800 | 0.0911 | 0.0885 | 10.27 | 0.078 | 0.0773 | 0.0826 |
| 1C | 10.82 | 0.1124 | 0.1006 | 0.0944 | 10.4.0 | 0.0968 | 0.090 | 0.088 |
| 1B | 11.02 | 0.0859 | 0.0913 | 0.0959 | 10.60 | 0.0782 | 0.0845 | 0.0854 |
| 2C | 11.22 | 0.116 | 0.1066 | 0.1043 | 10.85 | 0.0991 | 0.098 | 0.0954 |

3. VELOCITY DISTRIBUTIONS

Figure 3 presents the dimensionless velocity distributions at several cross-sections. All figures are plotted with the same scale.

Figure 3A (top left) shows a small velocity redistribution between the upstream flow (U/S) and the start of the shock waves (SW). Further, both figures 3B (top right) and 3C (bottom left) indicate a strong flow deceleration near the free-surface downstream of the shock waves : i.e., at $(SW1)_{z/W=0.05}$, $(SW2)_{z/W=0.05}$, $(SW2)_{z/W=0.05}$. Indeed, the shockwaves (also called oblique jumps) are associated with local energy dissipation and hence a loss of kinetic energy near the free-surface.

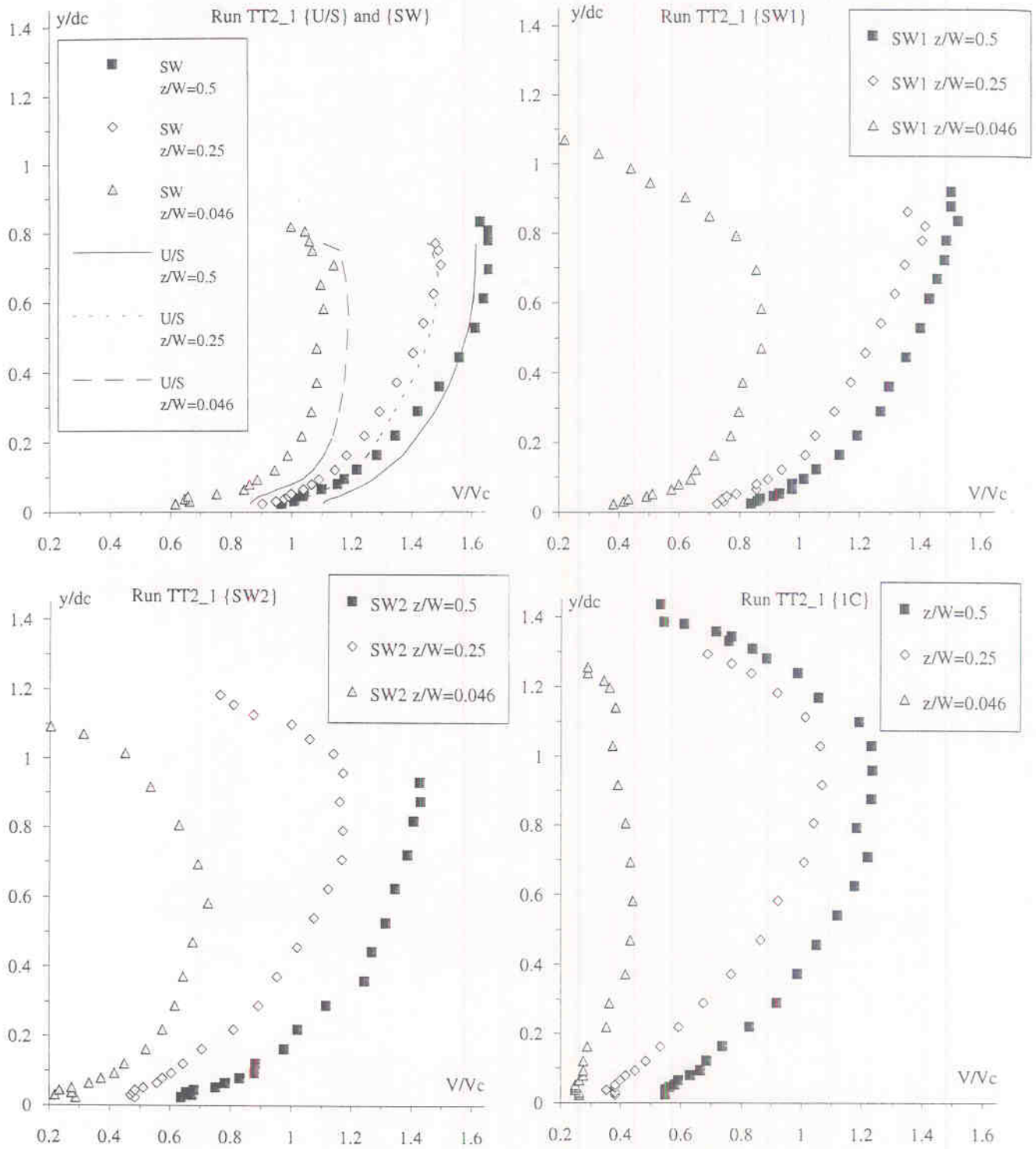
At the first wave crest (1C), a strong velocity deceleration is observed also next to the free-surface. Indeed, the shockwaves intersect at the first wave crest and a small "cockscomb" roller might take place. These processes enhance the energy dissipation at the free-surface and cause a local velocity reduction particularly on the centreline.

4. DISCUSSION

For the present series of experiments, the lateral shock waves occur for $Fr_1 > 1.2$ independently of the aspect ratio. Other researchers (FAWER 1937, IWASA 1955, IMAI and NAKAGAWA 1992) observed also lateral shock waves at undular hydraulic jumps. Visual observations indicate that the shock waves have a 'roller' form.

The importance of the lateral shock waves (or "Mach" waves) was highlighted by MONTES (1986) and CHANSON (1993). The crosswaves characterise a flow separation mechanism near the sidewalls. The sidewall boundary layers are subjected to an adverse pressure gradient (i.e. $\partial P/\partial x < 0$) and a flow separation is observed next to the free-surface (fig. 1). The lateral boundary layers force the apparition of critical conditions near the wall sooner than on the channel centreline. The shockwaves propagate then along the channel.

Fig. 3 - Velocity distributions at SW, SW1, SW2 and 1C



Legend :

- on the centreline ($z/W = 0.5$)
- ◇ at $z/W = 0.25$
- △ at $z/W = 0.046$

5. CONCLUSION

The three-dimensional characteristics of undular hydraulic jumps with fully-developed upstream flows have been investigated experimentally. The results are in agreement with earlier studies (FAWER 1937, CHANSON 1993). They confirm the importance of the lateral shock waves and their effects on the flow field.

Immediately upstream of the lateral shock waves, the free-surface is concave, and the pressure gradient is larger than hydrostatic. Downstream of the shock waves, the free-surface is convex, the pressure gradient is smaller than hydrostatic and a strong velocity deceleration is observed next to the free-surface.

ACKNOWLEDGMENTS

The author acknowledges the assistance of MM. B. TREVILYAN and L. TOOMBES, and the discussion with Dr J.S. MONTES (University of Tasmania, Australia).

REFERENCES

- CHANSON, H. (1993), *Research Report No. CE146*, Dept. of Civil Engineering, University of Queensland, Australia, Nov..
- FAWER, C. (1937), *Thesis*, Lausanne, Switzerland, Imprimerie La Concorde, 127 pages.
- IMAI, S., and NAKAGAWA, T. (1992), *Acta Mechanica*, Vol. 93, pp. 191-203.
- IWASA, Y. (1955), *Proc. 5th Japan Nat. Cong. for Applied Mechanics*, Paper II-14, pp. 315-319.
- LIGGETT, J.A. (1994). "Fluid Mechanics." *McGraw-Hill*, New York, USA.
- MONTES, J.S. (1986), *Proc. 9th Australasian Fluid Mech. Conf.*, Auckland, NZ, pp. 148-151.
- ROUSE, H. (1938). "Fluid Mechanics for Hydraulic Engineers." *McGraw-Hill*, New York, USA.

LIST OF SYMBOLS

- d flow depth measured perpendicular to the channel bottom (m);
- d_c critical flow depth(m) : in a rectangular channel $d_c = \sqrt[3]{q_w/g}$;
- Fr Froude number;
- g gravity acceleration : $g = 9.80 \text{ m/s}^2$ in Brisbane, Australia;
- P pressure (Pa);
- q_w discharge per unit width (m^2/s);
- V velocity (m/s);
- V_c critical flow velocity (m/s);
- W channel width (0.25 m);
- x distance (m) along the flume (fig. 1);
- y distance (m) from bottom measured perpendicular to the channel bottom;
- z horizontal distance (m) from wall;
- ρ_w water density (kg/m^3);

Subscript

- c critical flow conditions;
- 1 upstream flow conditions.